The effect of annealing time on microstructure and impact energy of stainless steel AISI 316L

Kožuh, Stjepan; Pavičić, Katarina; Ivanić, Ivana; Bizjak, Milan; Gojić, Mirko

Source / Izvornik: **Zavarivanje, 2021, 64, 79 - 86**

Journal article, Published version
Rad u časopisu, Objavljena verzija rada (izdavačev PDF)

Permanent link / Trajna poveznica: https://urn.nsk.hr/urn:nbn:hr:115:773465

Stjepan Kožuh, Katarina Pavičić, Ivana Ivanić,
Milan Bizjak, Mirko Gojić

ISSN 0044-1902
UDK 669.15.24.26
621.785
535.822
620.18

THE EFFECT OF ANNEALING TIME ON MICROSTRUCTURE AND IMPACT ENERGY OF STAINLESS STEEL AISI 316L

Keywords:
- stainless steel
- microstructure
- heat treatment
- annealing
- impact energy

Ključne riječi:
- nehrđajući čelik
- mikrostruktura
- toplinska obrada
- žarenje
- udarna radnja loma

Schlüsselwörter:
- Edelstahl
- Mikrostruktur
- thermisches Behandeln
- Glühen
- Schlagenergie

Author's address (adresa autora):

Stjepan Kožuh[1], Katarina Pavičić[2], Ivana Ivanić[1], Milan Bizjak[3], Mirko Gojić[1]

[1] University of Zagreb
Faculty of Metallurgy,
Aleja narodnih heroja 3, 44000 Sisak,
Croatia

[2] Master degree student
at University of Zagreb
Faculty of Metallurgy,
Aleja narodnih heroja 3, 44000 Sisak,
Croatia

[3] University of Ljubljana,
Faculty of Natural Sciences
and Engineering, Aškerčeva cesta 12,
1000 Ljubljana, Slovenia

Corresponding author *(e-mail address):*
kozuh@simet.unizg.hr

Received (primljeno):
2021-03-04

Accepted (prihvaćeno):
2021-03-31

Professional paper

In this work the results of microstructural analysis and impact energy testing of austenitic stainless steel AISI 316L were carried out. Investigations were performed before and after annealing at 850 °C. Annealing time in this investigation varied from 30 to 90 minutes. After annealing, the samples were cooled in room temperature air. Microstructural analysis of initial rolled and different annealed states was performed by optical microscopy (OM) and scanning electron microscopy (SEM) equipped with device for energy dispersive spectroscopy (EDS). Impact tests were performed on Charpy V-notch specimens at room temperature. Initial rolled state of investigated steel showed the presence of typical elongated polygonal grains austenite and delta ferrite while annealed states showed the presence and evolution of sigma phase in microstructure. Impact energy value of initial rolled state was 260 J and by increasing annealing time it decreases.

Strukovni članak

UTJECAJ VREMENA ŽARENJA NA MIKROSTRUKTURU I UDARNU RADNJU LOMA VISOKOLEGIRANOG ČELIKA KVALITETE AISI 316L

U ovom radu provedeni su rezultati analize mikrostrukture te ispitivanja udarne radnje loma austenitnoga nehrđajućeg čelika kvalitete AISI 316L. Ispitivanja su provedena prije i nakon žarenja na 850 °C. Vrijeme žarenja tijekom istraživanja mijenjalo se od 30 do 90 minuta. Nakon žarenja uzorci su ohlađeni na zraku pri sobnoj temperaturi. Mikrostrukturna analiza materijala prije toplinske obrade te nakon provedenih žarenja provedena je optičkom mikroskopijom (OM) kao i skenirajućim elektronskim mikroskopom (SEM) dodatno opremljenim EDS uređajem. Ispitivanja su provedena na sobnoj temperaturi na uzorcima za ispitivanje udarne radnje loma, Charpy V- utor. Početno valjano stanje ispitivanog čelika pokazalo je prisutnost tipičnih izduženih poligonalnih zrna austenita i delta ferita, dok žarena stanja pokazuju prisutnost i razvoj sigma faze u mikrostrukturi. Vrijednosti udarne radnje loma početnog stanja materijala bila je 260 J, a također je utvrđeno da se udarna radnja loma smanjuje s povećanjem vremena žarenja čelika.

Fachlicher Beitrag

DER GLÜHDAUEREINFLUSS AUF DIE MIKROSTRUKTUR UND AUFPRALLENERGIE DES EDELSTAHLS AISI 316L

In dieser Arbeit wurden die Ergebnisse der Mikrostrukturanalyse und der Schlagenergieprüfung von austenitischem Edelstahl AISI 316L durchgeführt. Die Untersuchungen wurden vor und nach dem Glühen bei 850 °C durchgeführt. Bei dieser Untersuchung variierte die Glühzeit von 30 bis 90 Minuten. Nach dem Glühen wurden die Proben in Luft bei Raumtemperatur abgekühlt. Die Mikrostrukturanalyse des anfänglichen Walzzustands und verschiedener geglühter Zustände wurde durch optische Mikroskopie (OM) und Rasterelektronenmikroskopie (REM) durchgeführt, die mit einer Vorrichtung zur energiedispersiven Spektroskopie (EDS) ausgestattet waren. Kerbschlagtests wurden an Charpy-V-Kerb-Proben bei Raumtemperatur durchgeführt. Der anfängliche Walzzustand des untersuchten Stahls zeigte das Vorhandensein typischer länglicher polygonaler Körner Austenit und Delta-Ferrit, während geglühte Zustände das Vorhandensein und die Entwicklung einer Sigma-Phase in der Mikrostruktur zeigten. Der Schlagenergiewert des anfänglichen Walzzustands betrug 260 J und nimmt mit zunehmender Glühzeit ab.

INTRODUCTION

Stainless steels (SS) are based on the binary Fe-Cr systems, the properties of which are modified by the additional alloying elements like nickel, molybdenum and manganese. Molybdenum is added usually to type 316 steel to enhance the corrosion properties, primarily the pitting and crevice corrosion resistance [1]. In the world`s total stainless steel production austenitic type steels take about 60% [2]. Austenitic stainless steels are often used in nuclear power plants, boilers, heat exchangers, chemical reactors etc. because their high resistance to corrosion and high temperature [3-5]. Also, stainless steel offers exceptional advantages for applications in construction [6]. Mostly stainless steels are used for construction as flat products and bars. Besides acceptable yield strength and tensile strength austenitic stainless steels are characterized by high impact energy and relatively low hardness. When considering the operational performance of austenitic stainless steel, the most important points to be taken into account are corrosion resistance, mechanical properties and the integrity of the welded joint in the case of welding these steels. Their high corrosion resistance resulted from for-

Table 1. Chemical composition of investigated austenitic stainless steel AISI 316L, wt.%
Tablica 1. Kemijski sastav čelika na kojem je provedeno istraživanje, AISI 316L

C	Mn	Si	Cu	V	Mo	Al	Cr	Ni	W	Ti	Nb	Fe
0.018	1.50	0.33	0.39	0.078	1.91	0.006	17.34	10.56	0.121	0.003	0.025	balance

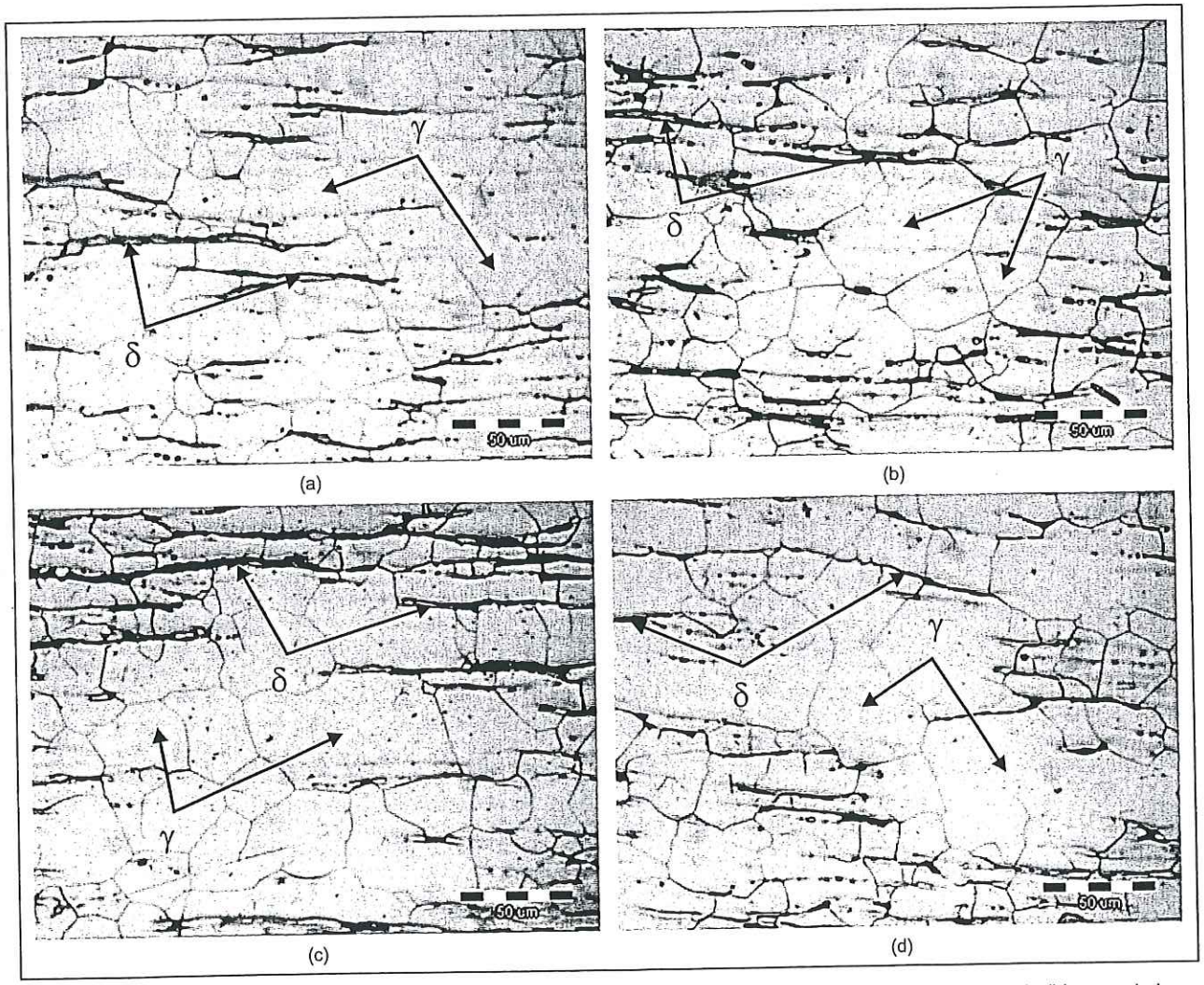

Figure 1. Optical micrographs of AISI 316L stainless steel in rolled (delivered) state (a), annealed state 850 °C/30 min (b), annealed state 850 °C/60 min (c), annealed state 850 °C/90 min (d); etching solution 1
Slika 1. Optička mikroskopija, nehrđajući čelik AISI 316L u valjanom (isporučenom) stanju (a), žareno stanje 850 °C/30 min (b), žareno stanje 850 °C/60 min (c), žareno stanje 850 °C/90 min (d); otopina za nagrizanje 1

mation of a continuous and protective surface oxide layer (passive film). This film is only a few nanometers thick and enriched in Cr (III) oxide/hydroxide species.

To reduce or prevent of microfissures in austenitic stainless steel, a minimum delta ferrite is required. Beneficial effect of delta ferrite is in dissolving more of

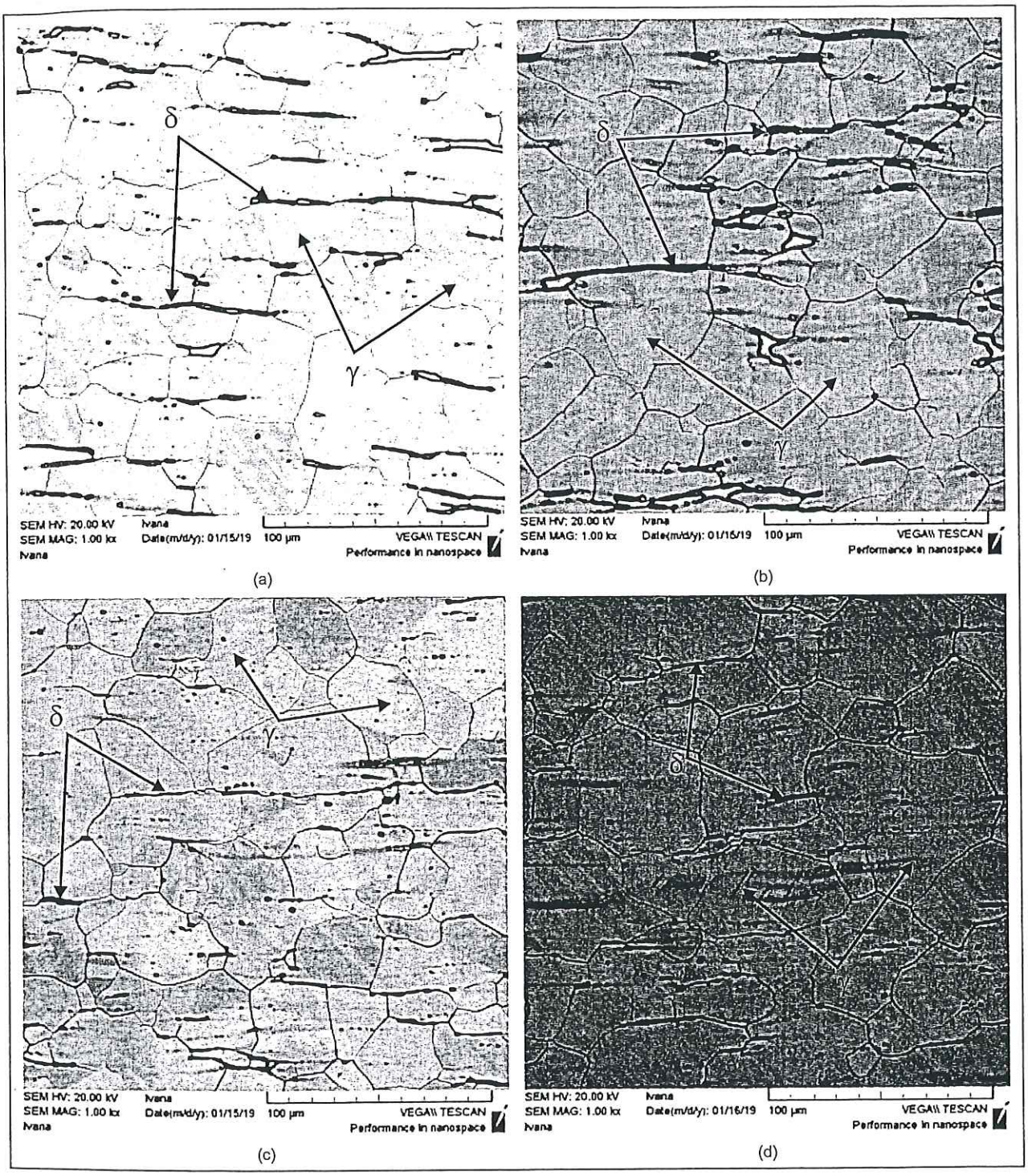

Figure 2. SEM micrographs of AISI 316L stainless steel in rolled (delivered) state (a), annealed state 850 °C/30 min (b), annealed state 850 °C/60 min (c), annealed state 850 °C/90 min (d); etching solution 1

Slika 2. SEM, elektronska mikroskopija, nehrđajući čelik AISI 316L u valjanom (isporučenom) stanju (a), žareno stanje 850 °C/30 min (b), žareno stanje 850 °C/60 min (c), žareno stanje 850 °C/90 min (d); otopina za jetkanje 1

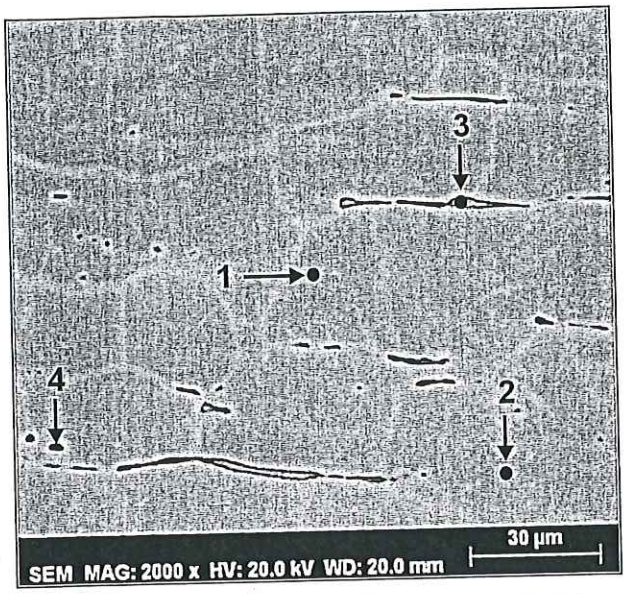

Figure 3. SEM micrograph of AISI 316L stainless steel in rolled (delivered) state with marked positions for EDS analysis; etching solution 1

Slika 3. SEM elektronska mikroskopija, nehrđajući čelik AISI 316L u valjanom (isporučenom) stanju s označenim položajima za EDS analizu; otopina za jetkanje 1

harmful elements such as sulfur, phosphorus and boron in austenite [7]. But, this ferrite can be transformed in sigma phase. Austenitic steels may undergo microstructural changes when they are exposed to elevated temperature for a shorter or longer period of time. Microstructural variations caused by heat treatment are responsible for changes in the mechanical properties and corrosion resistance. Usually, three intermetallic phases which can be occurred in austenitic stainless steels are sigma phase, chi phase and Laves phase [8-10]. The precipitation mechanism in austenitic stainless steels has been the subject of many investigations motivated by the detrimental effects of the precipitated phases on impact energy and corrosion resistance of steels [11-13]. Padilha et al. [11] and Sourmail [13] reported the precipitation of carbides ($M_{23}C_6$, MC, M_6C, M_7C_3), primary nitrides (MN, M = Zr, Ti, Nb and V), and secondary nitrides (M_2N, M = Cr, Fe) in austenitic stainless steels during thermal treatment (annealing) or welding. Dománková et al. [10] mentioned the following sigma phase composition in AISI 316 which observed after ageing at 800°C: 56–61%Fe, 21–26%Cr, 12–21%Mo and 1–5%Ni. As the sigma phase composition tends to vary it is difficult to define it by a formula but it is certain that it negatively affects on the steel properties.

The sigma phase has significant influence on properties of stainless steels and has been researched for some time [14]. Generally, the sigma phase forms via thermal ageing but also can be formed via radiation-induced segregation in FeCr alloys. Sigma phase is an intermetallic compound with a complex tetragonal crystalline structure and a typical sigma phase composition for the AISI 316L steel type is 44 % Fe - 29 % Cr - 8 % Mo. Sigma phase can be responsible for reduction in impact energy at room temperature.

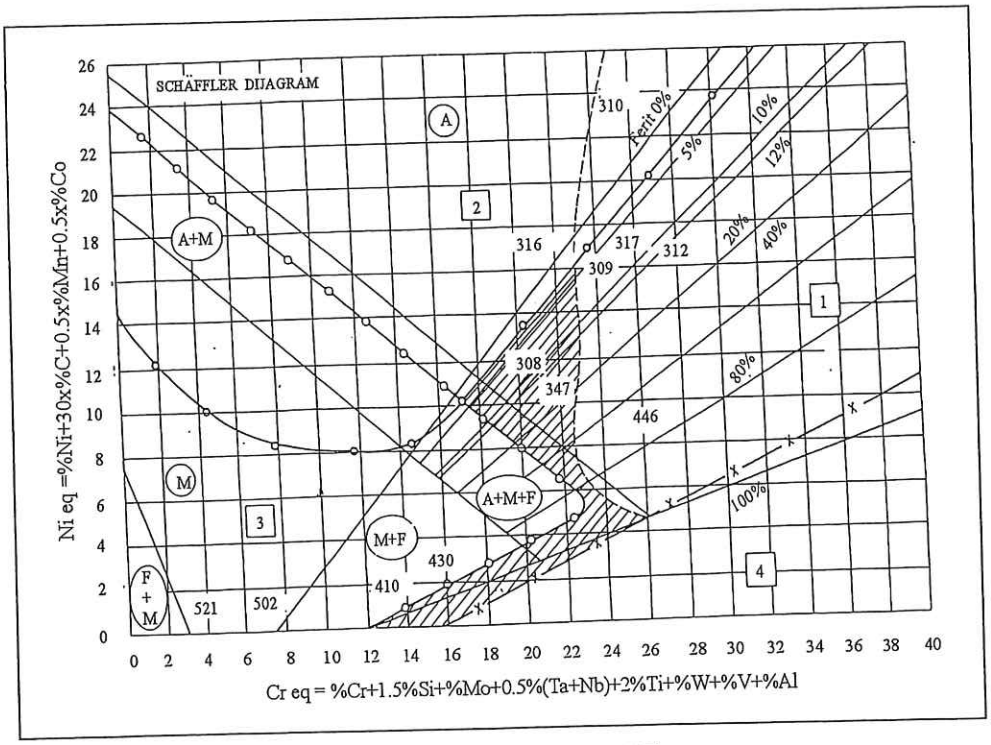

Figure 4. Schaeffler diagram [15]

Slika 4. Schaefflerov dijagram [15]

Table 2. Results of EDS analysis of different positions in as-rolled state AISI 316L stainless steel; positions marked at the Fig. 3
Tablica 2. Rezultati EDS analize različitih lokaliteta ispitivanja (1,2,3,4), valjano stanje nehrđajućeg čelika AISI 316L; lokaliteti su označeni na slici 3.

Positions	Chemical composition, wt.%					
	Fe	Cr	Ni	Mn	Mo	Si
1	67.19	16.50	11.74	2.00	2.24	0.33
2	67.81	16.44	11.82	1.88	1.77	0.27
3	67.53	16.66	11.75	1.97	1.84	0.26
4	67.87	16.87	11.19	1.77	2.07	0.23

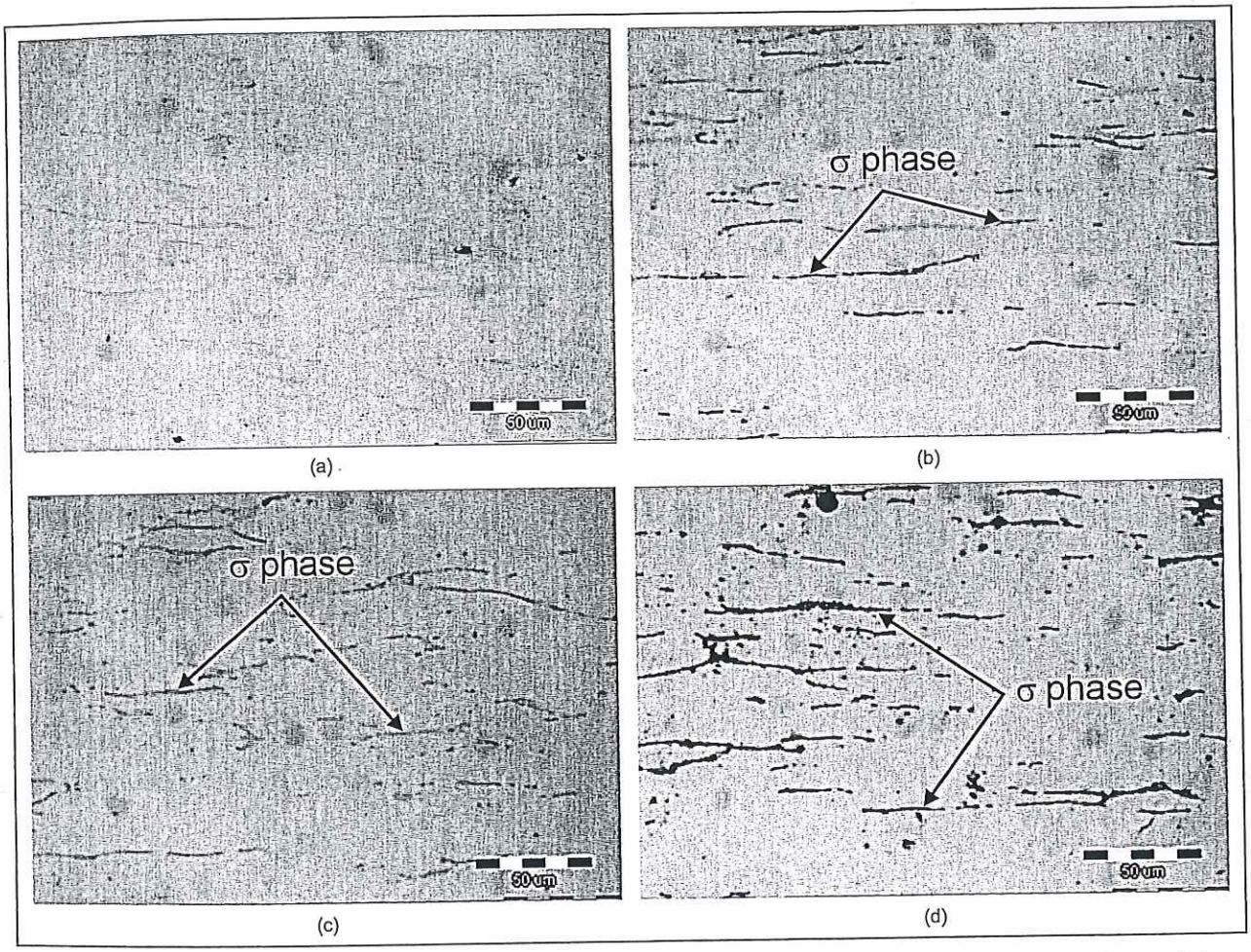

Figure 5. Optical micrographs of AISI 316L stainless steel in rolled (delivered) state (a), annealed state 850 °C/30 min (b), annealed state 850 °C/60 min (c), annealed state 850 °C/90 min (d); etching solution 2
Slika 5. Optička mikroskopija, nehrđajući čelik AISI 316L u valjanom (isporučenom) stanju (a), žareno stanje 850 °C/30 min (b), žareno stanje 850 °C/60 min (c), žareno stanje 850 °C/90 min (d); otopina za jetkanje 2

Due to AISI 316L stainless steel can be particularly useful at very high temperatures (e.g. in nuclear reactor) it becomes important to study the material microstructure and impact energy at elevated temperatures. The aim of the present work is to show possibility the sigma phase appearance and whether relative short annealing time (up to 90 minutes) can have an influence on microstructure and impact energy of austenitic stainless steel AISI 316L.

MATERIALS AND METHODS

The material used in this study was AISI 316L type stainless steel which was delivered in hot rolled state. The chemical composition of the investigated steel is listed in Table 1. Specimens for investigation were produced from steel plates of 15 mm thickness. Austenitic stainless steel AISI 316L was studied before and after heat treatment. Heat treatment was consisted from an-

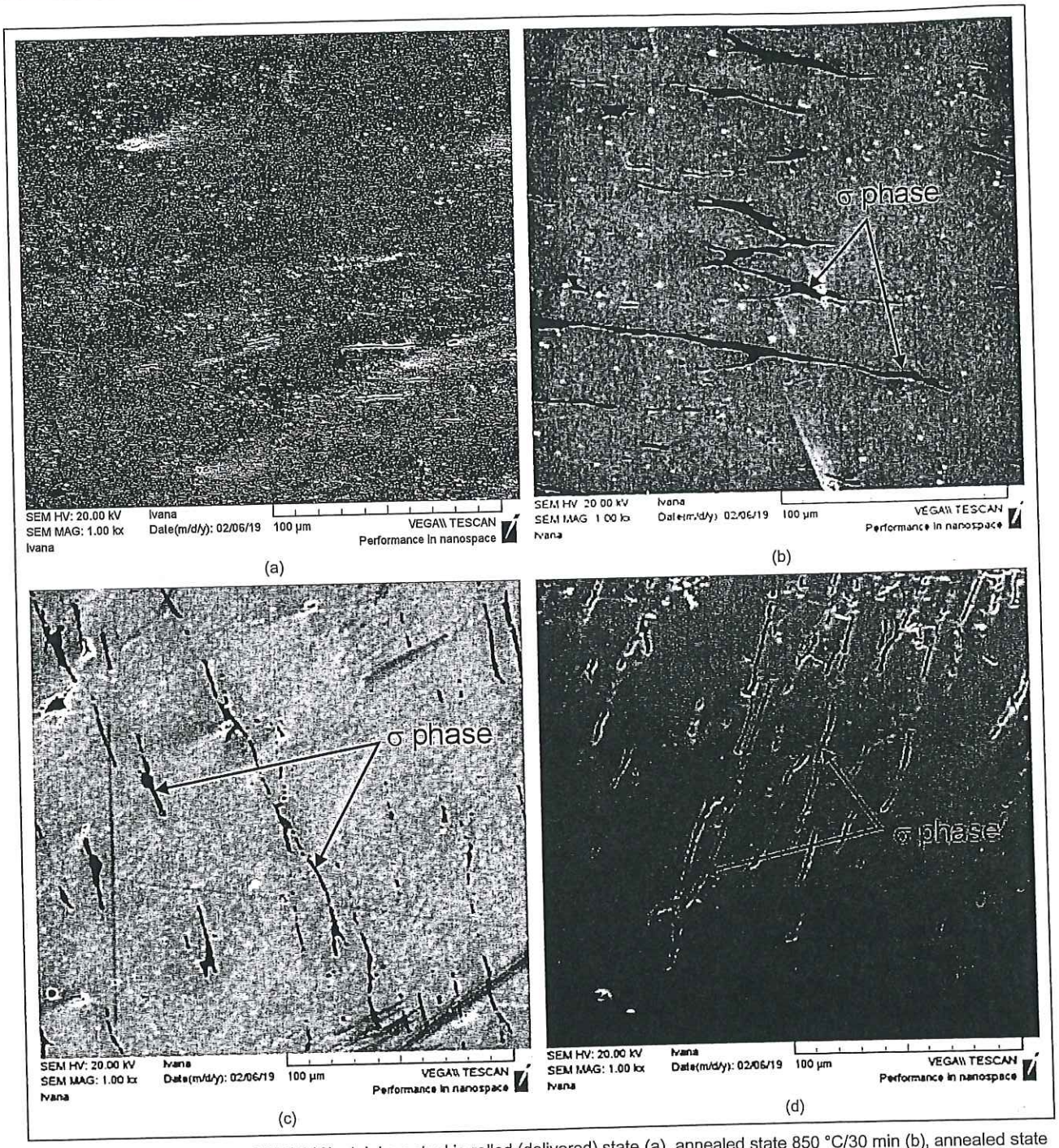

Figure 6. SEM micrographs of AISI 316L stainless steel in rolled (delivered) state (a), annealed state 850 °C/30 min (b), annealed state 850 °C/60 min (c), annealed state 850 °C/90 min (d); etching solution 2

Slika 6. SEM elektronska mikroskopija nehrđajući čelik AISI 316L u valjanom (isporučenom) stanju (a), žareno stanje 850 °C/30 min (b), žareno stanje 850 °C/60 min (c), žareno stanje 850 °C/90 min (d); otopina za jetkanje 2

nealing at 850 °C for 30, 60 and 90 minutes followed by cooling in the air. Microstructural analysis was carried out by optical microscopy Olympus GX 51 (OM) and scanning electron microscopy TESCAN VEGA 5136 MM (SEM) equipped with device for energy dispersive spectroscopy (EDS). Samples used for microstructural characterization were subsequently ground (papers grid 240-1200), polished (0.3 µ Al_2O_3) and electrolytically etched in two different solutions. To expose austenite boundaries, the etching solution 1 containing 60 ml HNO_3 and 40 ml water solution was used at 1V DC for 20 s. Sigma phase were identified with etching solu-

tion 2 composed from 56 g KOH in 100 ml water at 2V DC for 10 s. Impact tests were performed on Charpy V-notch specimens (7.5x10x55 mm) at room temperatures on device MLF System PSW 300.

RESULTS AND DISCUSSION

From the results of this paper it was possible to establish a correlation between the microstructure, impact energy and various annealing time at 850 °C for investigated AISI 316L stainless steel. The material in delivered (hot rolled) and thermal treated (annealed) state was microstructural characterized firstly after electrolytically etching to expose austenite boundaries (etching solution 1). Figs. 1-3 show a typical microstructure of the austenitic stainless steel of the present study. Optical micrographs (Fig. 1a) and SEM micrographs (Figs 2a and 3) of microstructure of rolled state exhibited typical elongated grains of polygonal austenite and delta ferrite. Stringers of delta ferrite are elongated in the direction of rolling. In AISI 300 series stainless steels, during casting firstly is formed delta ferrite, and then this ferrite transforms to austenite by diffusion of chromium and nickel between the phases. Chromium diffuses to the ferrite and nickel to the advancing austenite. The austenite grains nucleate and grow into delta ferrite grains. The presence of residual delta ferrite retained at room temperature can be ascribed to the slow diffusion of chromium and nickel. The microstructure, according to Schaeffler diagram (Fig. 4) [15], consisted of austenite and up to 10% of delta ferrite because the Cr_{eq}/Ni_{eq} ratio was 1.69 (Eqs. 1 and 2).

$$Cr_{eq} = \%Cr + 1.5\%Si + \%Mo + 0.5\%(Ta+Nb) + 2\%Ti + \%W + \%V + \%Al \quad (1)$$

$$Ni_{eq} = \%Ni + 30\%C + 0.5\%Mn + 0.5\%Co \quad (2)$$

It is generally held that up to 10% of delta ferrite in microstructure of austenitic stainless steel is an effective means of offsetting a grain boundary weakness that develops in austenite at high temperatures and leads to fissuring. From detailed analysis of optical and SEM micrographs (Figs. 1b, 1c, 1d and 2b, 2c, 2d) can be obtained similar microstructures in OM micrographs. In contrast, SEM micrographs show that increase in the annealing time results in a decrease content of elongated ferrite stringers. Annealing time was too short for visible changes at OM micrographs, probably. Fig. 3 show SEM micrograph of AISI 316L stainless steel in as-rolled state with marked positions for EDS analysis. The results of the EDS analysis (Table 2) show similar content of chromium (16.44-16.87 wt.%), nickel (11.19-11.82 wt.%), manganese (1.77-2.00 wt.%), molybdenum (1.77-2.24 wt.%), and silicon (0.23-0.33 wt.%) for all positions.

Also, the investigated steel in rolled and annealed state was microstructural characterized after electrolytically etching to expose sigma phase (etching solution 2). Figs. 5-7 show a microstructure of the austenitic stainless steel AISI 316L after etching in solution 2. The presence of sigma phase was observed. Optical and SEM micrographs show that the content of the sigma phase is increasing by increasing annealing time. In rolled (delivered) state (Figs. 5a and 6a) the sigma phase is not present since it only occurs by exposing the steel to high temperatures. Sigma phase is intermetallic phase which usually forms in the Fe-Cr systems at high temperatures (550-900 °C). The mechanism of sigma phase nucleation can be described by transformation of delta ferrite. Transformation of delta ferrite into sigma phase was a function of the chemical composition and the kinetics of its precipitation which was governed by the rate of diffusion sigma-forming elements, especially chromium and molybdenum. Fig. 7 show SEM micrograph of AISI 316L stainless steel in as-annealed 850 °C/90 min state with marked positions for EDS analysis. The results of the EDS analysis show similar content of manganese (1.96-1.98 wt.%), molybdenum (1.88-2.74 wt.%), and silicon (0.24-0.27 wt.%) for all analyzed positions. By contrast, the chromium content is higher at position 2 (Fig. 7, Table 3). Based on this it can be assumed that position 2 presents probably a sigma phase evolution with chromium content 21.42 wt.% and nickel content 6.79 wt.%.

Fig. 8 show the average values of impact energy testing of the investigated AISI 316L stainless steel before and after heat treatment (annealing). The values of impact energy are given as means of mostly three determinations. With a more detailed analysis of the impact energy values it can be seen that increasing annealing time (30-90 min) caused decreasing in impact energy. Before heat treatment impact energy value of AISI 316L stainless steel was 260 J. Heat treated state 850 °C/30 min/air have impact energy 224.5 J and it decreased to 166 J in heat treated state 850 °C/90 min/

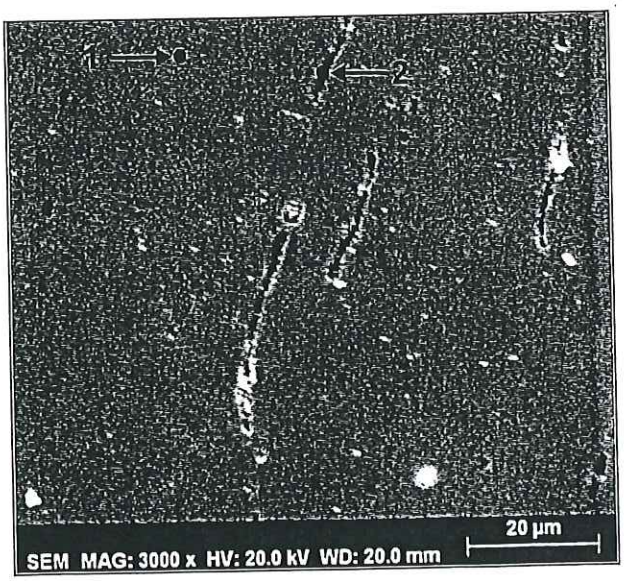

Figure 7. SEM micrograph of AISI 316L stainless steel in annealed state 850 °C/90 min with marked positions for EDS analysis; etching solution 2

Slika 7. SEM elektronska mikroskopija nehrđajući čelik AISI 316L u žarenom stanju 850 °C/90 min s označenim položajima za EDS analizu; otopina za jetkanje 2

Table 3. Results of EDS analysis of different positions in as-annealed state 850 °C/90 min; positions marked at the Fig. 6
Tablica 3. Rezultati EDS analize različitih lokaliteta ispitivanja u žarenom stanju 850 °C/90 min; položaji označeni na slici 6.

Positions	Chemical composition, wt.%					
	Fe	Cr	Ni	Mn	Mo	Si
1	68.86	15.81	11.23	1.96	1.88	0.27
2	66.82	21.42	6.79	1.98	2.74	0.24

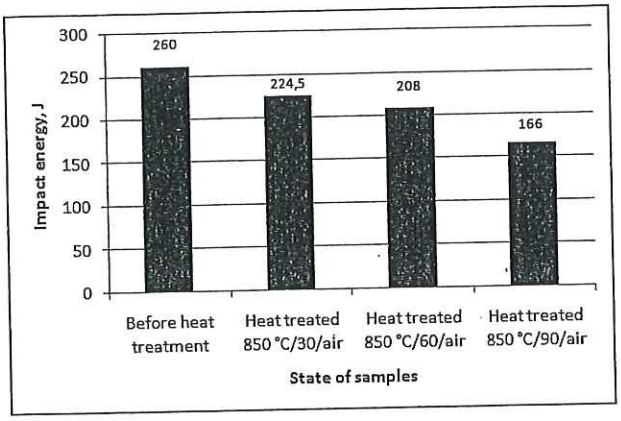

Figure 8. Impact energy vs. annealing time for stainless steel AISI 316L
Slika 8. Udarna radnja loma u odnosu na vrijeme žarenja, čelik AISI 316L

air. This decrease in impact energy can be related to microstructural changes i.e. occurrence and evolution of sigma phase by increasing annealing time.

CONCLUSIONS

Results of investigation the effect of annealing time on microstructure and impact energy of austenitic stainless steel AISI 316L suggest the following:

– Optical micrographs and SEM micrographs of microstructure of initial rolled state confirmed the presence of typical elongated polygonal grains of austenite and delta ferrite stringers.

– Increase in the annealing time from 30 to 90 minutes resulted in a decrease of elongated ferrite stringers content.

– EDS analysis showed similar content of chromium (16.44-16.87 wt.%), nickel (11.19-11.82 wt.%), manganese (1.77-2.00 wt.%), molybdenum (1.77-2.24 wt.%), and silicon (0.23-0.33 wt.%) for different positions in delivered rolled state.

– Optical and SEM micrographs showed the presence of sigma phase in annealed states. According to micrographs the content of the sigma phase is increasing by increasing annealing time.

– EDS analysis of annealed states showed position with higher chromium content (21.42 wt.%) and this position presents a sigma phase evolution, probably.

– Increasing annealing time from 30 to 90 minutes caused a decrease in impact energy. Impact energy value of stainless steel AISI 316L in initial rolled state was 260 J while after 90 minutes of annealing time impact energy decrease to 166 J. This decreasing can be result of occurrence and evolution of sigma phase during annealing.

This paper was presented at 18th International Foundrymen Conference "Coexistence of material science and sustainable technology in economic growth", Sisak, May 15th-17th, 2019.

Acknowledgements

This work was supported by the CRO-SLO bilateral scientific-research project „Analysis of fracture surfaces of microalloyed steels".

REFERENCES

[1] Z. Begum, A. Poonguzhali, R. Basu, C. Sudha, H. Shaikh, R.V. Subba Rao, A. Patil, R. K. Dayal, Studies of the tensile and corrosion fatigue behavior of austenitic stainless steels, Corrosion Science 53 (2011), 1424-1432.
[2] R.T. Loto, C.A. Loto, I. Ohijeagbon, Effect of heat treatment processes on the localized corrosion resistance of austenitic stainless steel type 301 in chloride/sulphate solution, Results in Physics 11 (2018), 570-576.
[3] L. Chang, M.G. Burke, F. Scenini, Stress corrosion crack initiation in machined type 316L austenitic stainless steel in simulated pressurized water reactor primary water, Corrosion Science 138 (2018), 54-65.
[4] S.S. Rezaei-Nejad, A. Abdollah-Zadeh, M. Hajian, F. Kargar, R. Seraj, Formation of nanostructure in AISI 316L austenitic stainless steel by friction stir processing, Procedia Materials Science 11 (2015), 397-402.
[5] R.K. Desu, H.N. Krishnamurthy, A. Balu, A.K. Gupta, S.K. Singh, Mechanical properties of austenitic stainless steel 304L and 316L at elevated temperatures, Journal of Materials Research and Technology 5 (2016)1, 13-20.
[6] N.R. Baddoo, Stainless steel in construction: A review of research, applications, challenges and opportunities, Journal of Constructional Steel Research 64 (2008), 1199-1206.
[7] Y. Cui, C.D. Lundin, Austenite-preferential corrosion attack in 316 austenitic stainless steel weld metals, Materials and Design 28 (2007), 324-328.
[8] Y. Song, N.A. Mcpherson, T.N. Baker, The effect of welding process on the Chi phase precipitation in as-welded 317L weld metal, ISIJ International 36 (1996)11, 1392-1396.
[9] I. Hrivňák, Metallography of austenitic and dual phase stainless steels, Acta Metallurgica Slovaca 10 (2004), 91-102.
[10] M. Dománková, V. Magula, Study of grain boundary structure on precipitation in 316 austenitic stainless steel, Acta Metallurgica Slovaca 10 (2004), 234-238.
[11] A. F. Padilha, R. L. Plaut, P. R. Rios, Annealing of cold-worked austenitic stainless steels, ISIJ International 43 (2003)2, 135-143.
[12] D. N. Wasnik, G. K. Dey, V. Kain, I. Samajdar, Precipitation stages in a 316L austenitic stainless steel, Scripta Materialia 49 (2003)2, 135-141.
[13] T. Sourmail, Precipitation in creep resistant austenitic stainless steels, Materials Science and Technology 17 (2001)1, 1-14.
[14] K.H. Lo, C.H. Shek, J.K.L. Lai, Recent developments in stainless steels, Material Science and Engineering R 65 (2009), 39-104.
[15] M. Gojić, Tehnike spajanja i razdvajanja, Metalurški fakultet, Sveučilište u Zagrebu, Sisak, 2003.